



# Defect size estimation and analysis of the path of rolling elements in defective bearings with respect to the operational speed

Alireza MOAZENAHMADI<sup>1</sup>; Dick PETERSEN<sup>1</sup>; Carl HOWARD<sup>1</sup>; Nader SAWALHI<sup>2</sup>

<sup>1</sup>The University of Adelaide, Australia

<sup>2</sup>Prince Mohammad Bin Fahd University, Kingdom of Saudi Arabia

## ABSTRACT

This paper investigates and explains the path of a rolling element in the defect zone and the nature of the entry and exit events of the two main features that appear in the vibration signal of a defective bearing. Vibration response and contact forces between the rolling elements and bearing raceways are simulated and compared with the measured vibration signals. Assumptions used in previous defect size estimation methods in describing the path of the rolling elements in the defect zone, are investigated and some discrepancies are identified. These analyses are essential to develop defect size estimation algorithms. Therefore, the defect size estimation results of the existing signal processing algorithms often contain significant errors and are biased for different operational speeds. A method to validate the explanations offered by this study for the true path of rolling elements in the defect zone is proposed. This method can be used for defect size estimations for defective bearings. The research shows that this method is more accurate and less biased for speed when compared with existing methods.

Keywords: Rolling element bearing, spall, vibration model, defect size, contact forces

## 1. INTRODUCTION

Rolling element bearings are widely used in rotary machinery and the failure of bearings is the most common reason for machine breakdowns. Effective bearing condition monitoring systems should be able to detect and estimate the size of defects in bearings correctly at early stages of the defect development to enable remedial actions to be taken. Therefore, appropriate models and signal processing algorithms to track the growth of defects are essential.

Defects in bearings are commonly categorised into localized and distributed defects. Distributed defects, such as waviness, surface roughness, or off-size rolling elements, are usually the result of manufacturing errors (1, 2). Localized defects are often initiated by insufficient lubrication film between the contact surfaces. This causes metal-to-metal contact between the rolling elements and the raceways, which in turn generates stress waves, leading in time to the formation of sub-surface cracks. The large forces in bearings cause the sub-surface cracks to grow into surface defects. This phenomenon is called pitting or spalling (3). This paper considers the vibrations and contact forces generated in bearings with raceway spalls also known as line-spalls.

Previous studies on the vibration signature of defective bearings with raceway spalls show that passage of a rolling element over the spall generates two main components. The first component, which has low frequency content, results from the entry of a rolling element to the spall. The second component, which has higher frequency content, results from the impact of a rolling element to the trailing edge of the spall (4-7). Several defect size estimation methods were previously suggested based on the extraction of the time separation between these two components from the vibration signal (4, 8). These algorithms are based on the assumptions which directly affect the outcome results. In order to enhance the vibration signature of these two events, signal processing algorithms are suggested.

This study investigates the generally accepted assumptions by previous studies and has identified some discrepancies in previous works describing the path of rolling elements in the defect zone and identifying the corresponding points in the vibration response to the entry and exit events.

## 2. PREVIOUS WORK

### 2.1 Vibration of localised defective rolling element bearings

Figure 1 illustrates a diagram of a defective rolling element bearing with a line-spall defect on the outer raceway. A typical measured vibration signal due to such a defect is shown in Figure 1b. It has been shown by previous experimental studies that the entry of a rolling element into a line-spall defect produces a vibration signal with low frequency content (4, 9). Moreover, the exit of the rolling element excites a much broader range of frequencies including the high frequency bearing resonances. These resonances are excited by the impact of the rolling element mass on the exit point of a defect, as well as the parametric excitations caused by rapid changes in the bearing stiffness which occur when the rolling element re-stresses between the raceways (5). The high frequency event observed in experimental results (7, 9) often appears to have been caused by multiple impacts rather than a single impact. Simulation results of defective bearings presented by Singh (6) indicate that the multiple impacts occur when the rolling element successively impacts on the inner and outer raceways as it re-stresses at the exit point.

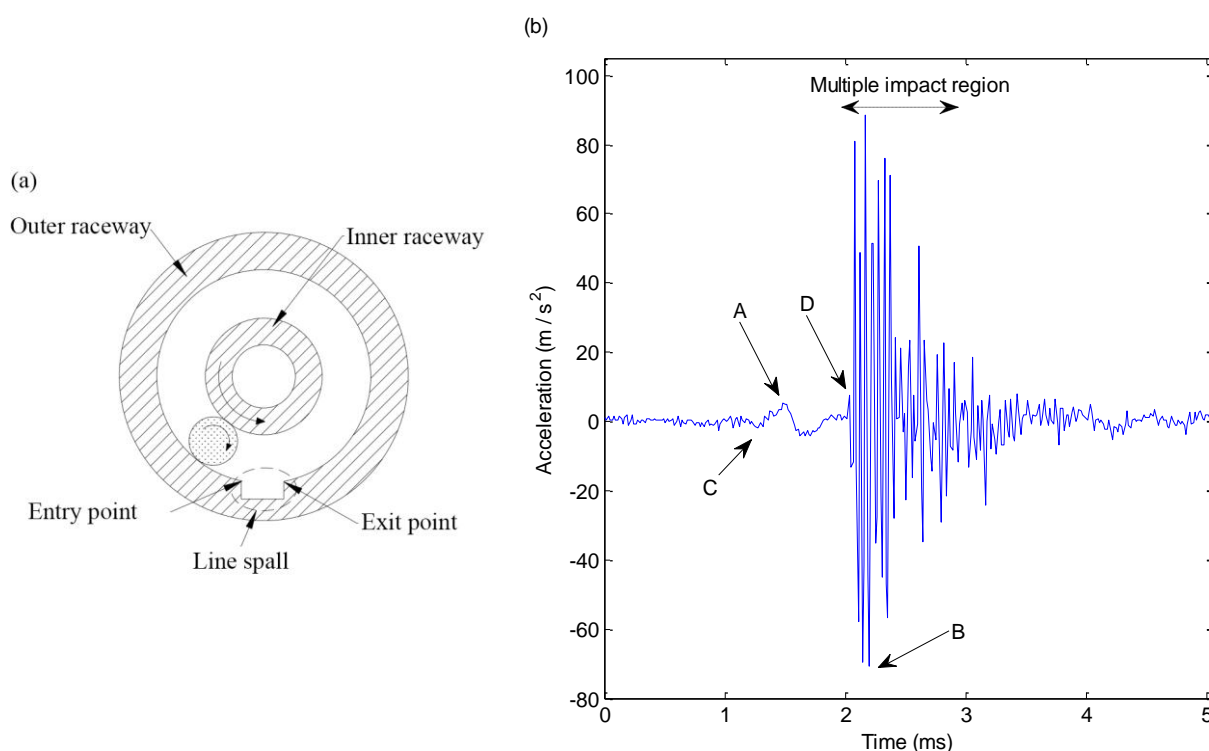


Figure 1: (a) Diagram of a rolling element travelling into a line-spall defect located on the outer raceway. (b) A typical measured vibration response. Points A and B are typical entry and exit points suggested by previous studies (4, 8), whereas the analysis in this paper shows that points C and D are the entry and exit points.

It is generally accepted that for a bearing with a line-spall defect, the high frequency impulsive event in the measured vibration response corresponds to the excitation of high-frequency bearing resonant modes, which occur when the centre of a rolling element is halfway through the defect. The defect size estimation methods which are based on detecting the time separation between the low and high frequency events, assume that the spatial separation between the events on the vibration response corresponds to half the defect size (4). Some signal processing algorithms designed to enhance and extract the entry and exit features in the vibration response are suggested in (4, 8). However, these studies did not investigate the actual path of a rolling element and the exact corresponding points in the vibration response to the entry and exit events. These researchers assumed that point A, shown in Figure 1, corresponds to the entry point, while one of the largest high frequency responses, shown as point B in Figure 1, in the multiple impact region, corresponds to the exit point of a defect. However, the experimental results of these defect size estimation algorithms are biased with speed (4, 8).

Simulations presented in this paper have investigated the assumptions used in the defect size estimation methods described earlier and have identified some discrepancies in describing the path of the rolling elements into a defect and the corresponding features on the vibration response to the entry and exit events. These discrepancies are contributing to the inaccuracy and bias in the defect size estimation algorithms proposed previously. This paper has demonstrated that the exit impacts do not necessarily happen midway through a defect. Moreover, the corresponding time at which the roller enters and exits the fault zone is shown in the vibration response at C and D respectively, as shown in Figure 1.

## 2.2 Vibration models for line-spall defects

Numerous multi-body dynamic models have been developed for modelling line-spall defects (10-16) which do not consider the mass and finite size of the rolling element. In these models, the path of a rolling element is modelled such that its centre follows the geometry of the modelled defect. Harsha (17-20) has considered the mass and centrifugal forces acting on a rolling element but not the finite size of the rolling element in his multi-body dynamic model. This model was initially developed to predict the vibration response of defective bearings with distributed defects (21). Later on, the model was improved to include the mass of the rolling elements to predict the nonlinear dynamic behavior of a rolling element bearing due to waviness and unbalanced rotor support (17-20). The improved version of the model was further modified by Tadina (16) to predict the vibration response of bearings with localized spall defects on raceways. All of the aforementioned models are designed for defects with curvatures larger than the curvature of the rolling element which maintains the contact between the raceways in the load zone. Therefore, none of the above multi-body dynamic models are suitable for modelling the path of a rolling element in the defect zone of a defective bearing with a line-spall defect.

Recently, a more comprehensive multi-body dynamic model was developed by Moazen Ahmadi et al. (7, 22) which considers the mass and centrifugal forces acting on rolling elements and, more importantly, the finite size of the rolling element. They showed that in order to predict the path of a rolling element and the corresponding features in the vibration response correctly, it is crucial to include the finite size of rolling elements when modelling localised defects. More details of the multi-body dynamic model used in this paper can be found in reference (7, 22).

## 3. TEST EQUIPMENT

The test rig data considered in this study is part of a previous study into the development of spall size estimation techniques for defective bearings (4). The test rig includes a fan disk with 19 blades fitted on a shaft which is supported by two Nachi 2206GK double row self-aligning ball bearings. These bearings have 14 balls on each row, a pitch diameter of 45mm, a ball diameter of 8mm, and a contact angle of  $0^\circ$ . The balls are retained in a staggered arrangement by a single cage, with the angular offset between the two rows equal to half the angular ball spacing on the individual rows. The shaft is driven by a motor via a V-belt and the rotational speed is controlled using a variable voltage and frequency drive. Line-spalls of varying sizes were machined on the outer raceway, and the vibration response was measured at various speeds using an accelerometer. A detailed description of the test rig and the defects that were inserted can be found in reference (4).

## 4. MEASUREMENTS AND SIMULATIONS

### 4.1 Model description and analysis

This section presents a comparison between simulated and experimental vibration results. The aims of the simulations are to show that the model can predict characteristics observed in the measured vibration response, and investigate the path of a rolling element in the defect zone. The nonlinear multi-body dynamic model introduced in Section 2.2 was implemented to simulate the measured vibration response of the bearing described in Section 3. The measured response considered here was sampled at 65,536 Hz. The natural frequency and damping ratio of the high-frequency resonant mode included in the model were set to 20 kHz and 3%, respectively. This corresponds to a high-frequency bearing resonant mode observed in the measured vibration response. A static load of 100 N and a clearance of 3  $\mu\text{m}$  were used in the model. The parameter values used in the model are chosen according to references (5, 7, 10, 11) and listed in Table 1.

Table 1: Model parameter values used for simulation

Load-deflection factor between a ball bearing and the outer race way	10.3 GN/m <sup>1.5</sup>
Load-deflection factor between a ball bearing and the inner race way	18.9 GN/m <sup>1.5</sup>
Support stiffness	8 MN/m
Support damping	10%
Mass of inner race and the shaft	2 kg
Mass of outer race	3 kg
Viscous damping constant	75 N s/m

Figure 2a shows 0.025 seconds of the acceleration data that was experimentally measured on the test bearing at the speed of 800 rpm and 100 kN static radial load. The simulated acceleration response is included in Figure 2b. The experimental data was low-pass filtered at 22 kHz as the bearing resonances at higher frequencies are not considered in the model.

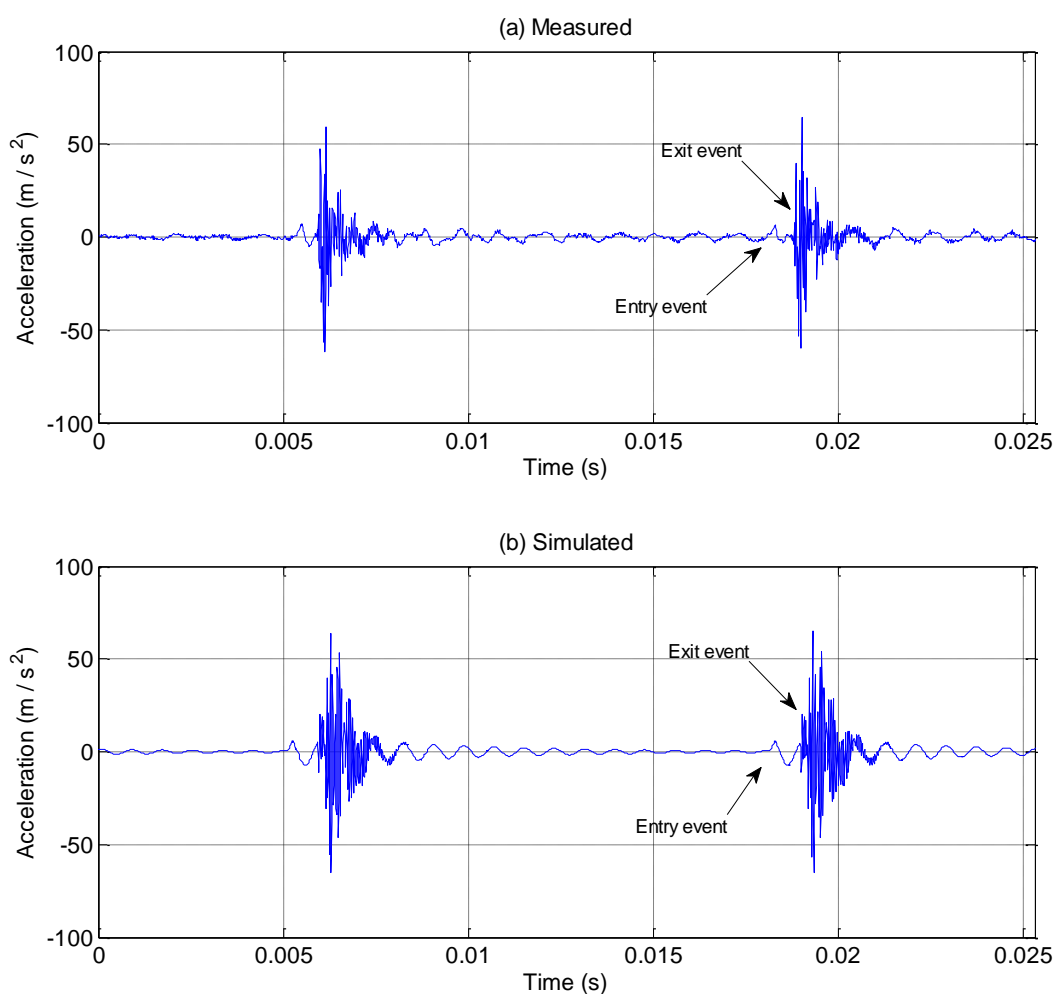


Figure 2: 0.025 seconds of bearing vibration response at 800 rpm with 1.2mm defect size(a) Measurement vibration response of the test bearing (b) Simulated vibration response.

Figure 3a shows a zoomed-in section of the signals presented in Figure 2, where the zoomed-in section corresponds to the period of time in which a roller approaches and leaves the defect on the defective raceway. Figure 3b shows the path of the radial position of the rolling element. In Figure 3b, the small difference between the roller path and the defect geometry, outside the defect zone, is the roller contact deformation. Figure 3 a and b show that at approximately 0.1244s, when the roller enters

the defect, low frequency vibration is generated in both the experimentally measured and simulated vibration.

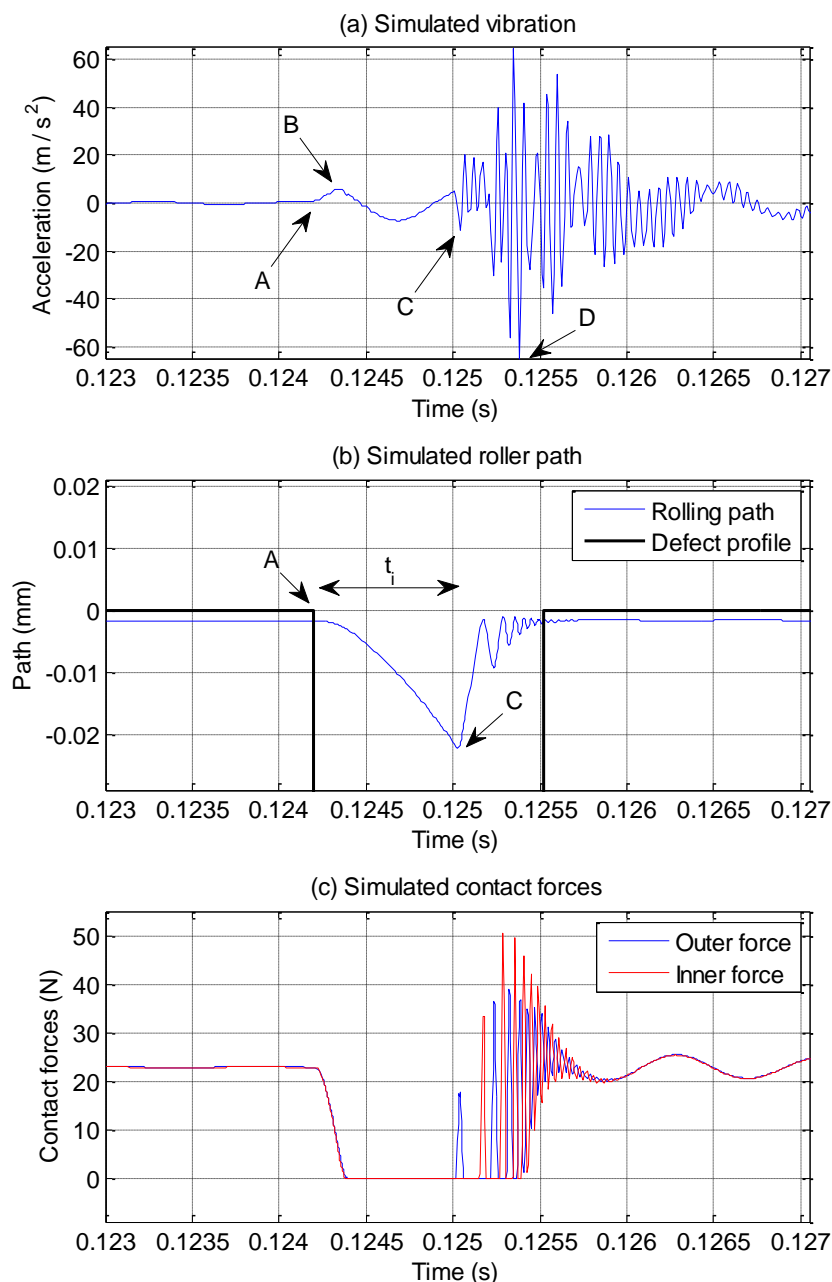


Figure 3: (a) Simulated vibration response of the test bearing at 800 rpm with 1.2mm defect size (b) Simulated path of the deformed contact point on the circumference of the rolling element as it travels through the defect zone.  $t_i$  is the time to impact (c) Simulated inner and outer contact forces acting on the same rolling element.

The key vibration characteristics observed in the simulated and measured results are listed and analysed below.

**Rolling element entry:** The entry of the rolling element into the defect generates predominantly low frequency content in the vibration response. This low frequency vibration is due to the gradual de-stressing of the rolling element, which starts at entry point A, and ends when the rolling element hits the exit point at C as shown in Figure 3a. The travel time of the centre of the roller from point A to C is shown as  $t_i$  in Figure 3b. The entry of the rolling element into the defect during time  $t_i$  can be considered as two events. The first is the entry transient (A-B) that is the gradual de-stressing of the

rolling element as it enters the defect, and lasts until the contact forces acting on the rolling element become zero as it loses contact with both raceways. The gradual decay of the contact forces can be seen in Figure 3c. During this stage, the load has to be redistributed amongst the other rolling elements in the load zone, consequently, an increase in the vibration response occurs. As the number of the load carrying rolling elements decreases, the bearing assembly stiffness decreases. As this reduction is gradual, only low frequency modes of the system will be excited, which results in the low frequency event in the vibration signal. The second event is the free-drop (B-C) of the rolling element into the defect, shown in Figure 3a. During this process, the rolling element has no contact with the raceways and it carries no load. Therefore, the only acting forces on the rolling element at this stage are the mass and the centrifugal forces.

**Rolling element exit:** This event is mostly associated with the excitation of high frequency modes of the bearing assembly. The exit of the rolling element from the bearing defect can be considered as the two events. The first event is that the rolling element strikes the exit point of the defect for the first time. The high-frequency event in the vibration response observed at point C, as shown in Figure 3a, is associated with this event, where the rolling element has to change direction suddenly. This abrupt change in the direction of movement causes a step change in velocity and generates an impulse in the acceleration signal, which excites the high frequency resonance mode of the bearing assembly that is included in the proposed model. Secondly, when the rolling element re-stresses between the raceways at the defect exit, multiple impacts occur as it alternately strikes the outer and inner raceway and re-stresses back to its normal load carrying capacity (23). The multiple impacts at the exit of the defect can be seen in the experimental results in Figure 1b, and have also been observed in experiments presented in previous studies (6, 7). It should be noted that the first impact to the exit point of the defect is not necessarily the impact with the maximum amplitude among the multiple impacts. The result suggests that the observed maximum point of the high frequency excitation often occurs after several oscillations from the first impact of the rolling element to the exit point. The maximum amplitude of the high frequency excitation might be the result of the summation of different excited natural frequencies or superposition of excited high frequency modes on top of the low frequency component excited as the result of the exit transient of the rolling element.

The outcome of the simulation has revealed the following discrepancies in assumptions made by previous studies which were used in defect size estimation algorithms. These findings are essential to develop accurate defect size estimation algorithms and explain the inaccuracy of the previous algorithms:

- It was generally accepted that the first peak of the low frequency oscillation on the vibration response corresponds to the time when a rolling element hits the entry point to the defect. Thus the peak of the low frequency oscillation was used in previous defect size estimation methods. However, it is shown that the corresponding point on the vibration response to the defect's entry point is the rising point of the first low frequency oscillation.
- It was assumed that the rolling element strikes the exit point when the center of a rolling element is mid-way through the defect. However, it is shown that the both contact forces acting on a rolling element become zero long before the roller reaches the exit point.
- It was assumed that the highest peak among the high frequency responses in the multiple impact region corresponds to the defect's exit point. However, it is shown that the first high frequency oscillation corresponds to the first exit impact.

## 5. PROPOSED METHOD TO ESTIMATE THE DEFECT SIZE

### 5.1 Formulation

In this section, the analysis presented in the previous section is used to develop a method to estimate the bearing's defect size. The low frequency event on the vibration signal is a good indication of the point of entry (where the centre of the rolling element reaches the exit point). However, when the centre of a rolling element reaches the exit point, finding the exact exit impact event among the multiple exit impacts is a challenging task. Nevertheless, finding the point on the vibration response which corresponds to the first impact of a roller to the defect's exit point is relatively easy. In order to estimate the defect size successfully, it will be useful to consider the overall estimation of the size of the defect to be the sum of two length estimations. Figure 4 shows a schematic of the travel path of a rolling element in the defect zone and the two lengths to be estimated,  $L_1$  and  $L_2$ . The first is the estimation of the length to which the centre of a rolling element travels from the point of entry (point

A on the Figure 4) and the first impact to the exit point (point C on Figure 4). The second length estimation is the length between the impact point on the circumference of the rolling element and the centre of the rolling element.

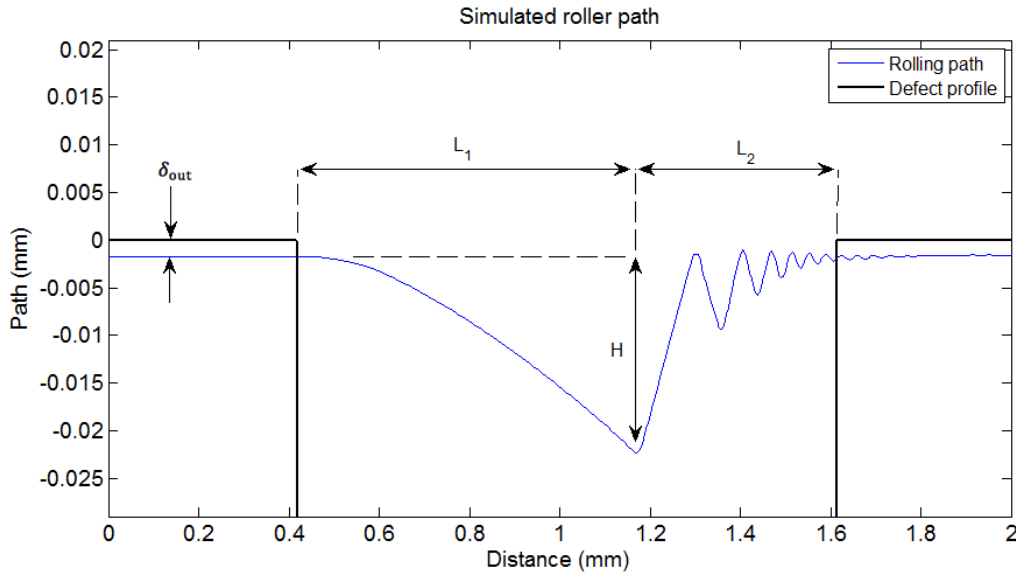


Figure 4: Schematic of the travel path of a rolling element in the defect zone. and the two lengths to be estimated,  $L_1$  and  $L_2$  are the two lengths to be estimated,  $H_i$  is the vertical relative movement of a rolling element at the time of first impact and  $\delta_{out}$  is the maximum relative deflation between a rolling element and the outer race in the load zone

The travel length to the first impact  $L_1$  can be calculated by

$$L_1 = \sin(t_i \times \omega_c) \times d, \quad (1)$$

where  $\omega_c$  (Hz) is the rotational speed of the cage,  $d$  is the radius of the outer raceway and  $t_i$  is the travel time of the centre of a rolling element from the point of entry to the first impact.  $t_i$  is the measured time between the rising point of the first low frequency oscillation and the first high frequency oscillation on the vibration response.

The length between the impact point on the circumference of the rolling element of its centre  $L_2$  can be determined geometrically by relating the vertical relative movement of a rolling element  $H_i$  at the time of first impact, shown in Figure 4, to the dimensions of the rolling elements as

$$L_2 = r_b \times \cos(\arcsin(r_b - (H_i + \delta_{out})/r_b)), \quad (2)$$

where  $r_b$  is the radius of a rolling element and  $\delta_{out}$  is the maximum relative deflation between a rolling element and the outer race in the load zone.  $\delta_{out}$  depends on the curvature of the rolling elements and raceways, and the applied load (3). The path of the centre of a rolling element after losing contact with both raceways depends on the mass of a rolling element and the rotational speed of the shaft (7, 22). Therefore, function  $H(t)$ , which provides the vertical relative movement of a rolling element at a given time  $t$ , can be obtained by simulating a large defect for different speeds and creating a polynomial curve fit of the path of a rolling element in the defect zone. The function  $H(t)$  can be used to estimate  $H_i$  by measuring  $t_i$  from the experimental vibration measurements.

## 5.2 Validation

In this section, the proposed method in Section 5.1 is used to estimate the size of a defect in bearings with 0.6mm and 1.2mm defects described in Section 3. In order to capture the vertical distance, the vertical relative movement of a rolling element  $H(t)$ , simulation of the path of a rolling element for a similar bearing but with larger defect of 2.4mm is carried out. Figure 5 illustrates the results of polynomial curve fit results of order 4 for 0.06s of the dropping path of a rolling element in

the defect zone for different speeds.

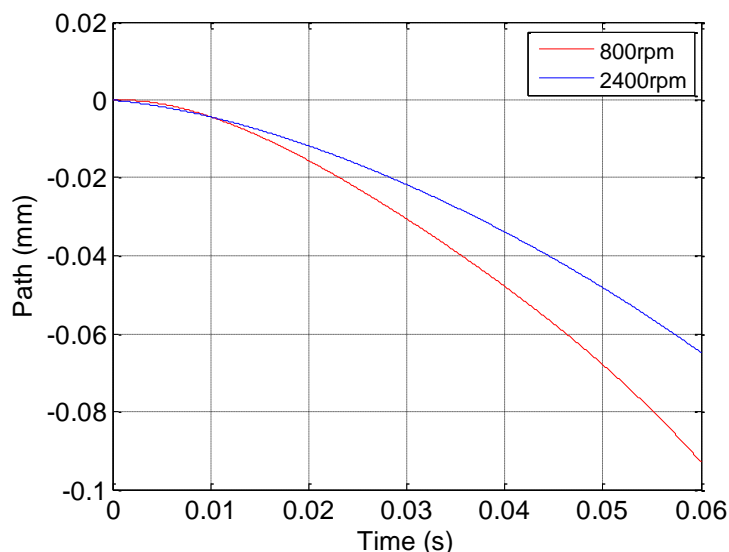


Figure 5: Polynomial curve fit results of order 4 for 0.06s of the traveling path of a rolling element in the defect zone for different speeds

The mean and the standard deviation for a number of events on the vibration response of the two test bearings (with 0.6mm and 1.2mm defect sizes) for different speeds were estimated using the procedure described in section 5.1 and the polynomial curve fit functions obtained from the simulations of a defective bearing with 2.4mm defect size for different speeds. These results are compared against the defect size estimation results using the method suggested by Sawalhi and Randall on same bearings (4) in Figure 6. Note that results based on the study presented in this paper are generally more accurate and also less biased with speed.

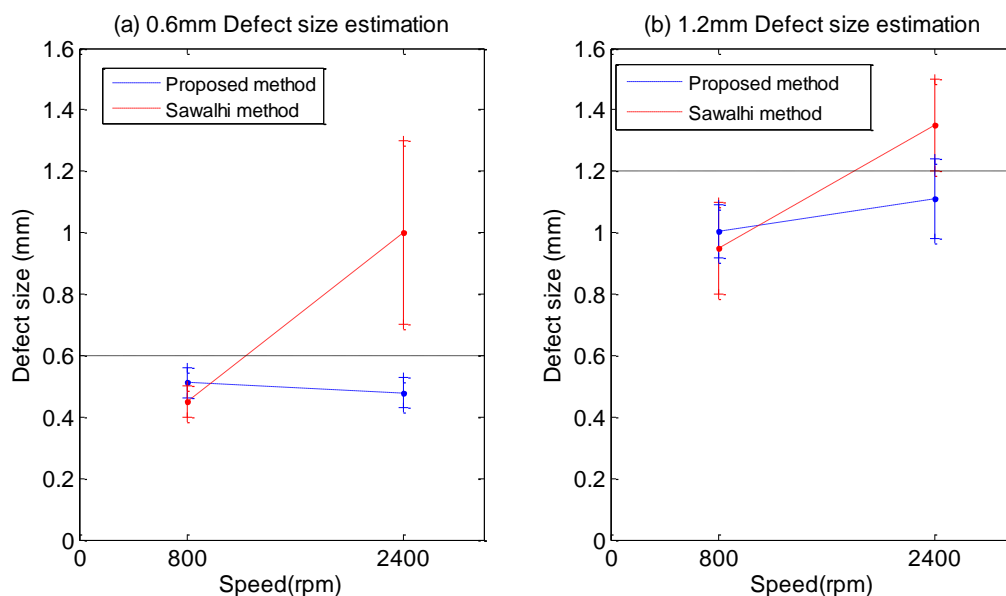


Figure 6: Comparison between the estimated mean and standard deviation of outer race defects using the method suggested by Sawalhi and Randall (4) and the proposed method in this paper for: a) 0.6mm defect and b) 1.2mm defect

## 6. CONCLUSIONS

This paper has demonstrated the importance of understanding the path of rolling elements in the defect zone for developing an algorithm to estimate the size of a bearing defect. The discrepancies in

the assumptions made by previous studies are identified by simulations presented in this paper. The path of a rolling element in the defect zone are predicted and related to the experimental vibration measurements. A method for defect size estimation based on these analyses is presented which has the capacity to estimate the bearing's defect size more accurately which is less bias with operational speed. Moreover, experimental estimation of the defect size using the vibration signal validates the analysis of the path of a rolling element in the defect zone in this paper.

## REFERENCES

1. Su YT, Lin MH , Lee MS. The effects of surface irregularities on roller bearing vibrations. *Journal of Sound and Vibration*. 1993;165(3):p. 455-466.
2. Sunnersjö C. Rolling bearing vibrations-the effects of geometrical imperfections and wear. *Journal of Sound and Vibration*. 1985;98(4):p. 455- 474.
3. Harris TA. *Rolling bearing analysis*. USA: Wiley; 2001.
4. Sawalhi N , Randall RB. Vibration response of spalled rolling element bearings: Observations, simulations and signal processing techniques to track the spall size. *Mechanical Systems and Signal Processing*. 2011 4//;25(3):p. 846-870.
5. Petersen D, Howard CQ, Sawalhi N, Moazen Ahmadi A , Singh S. Analysis of bearing stiffness variations, contact forces and vibrations in radially loaded double row rolling element bearings with raceway defects. *Mechanical Systems and Signal Processing*. 2015;50-51:p.139-160. <http://dx.doi.org/10.1016/j.ymssp.2014.04.014>
6. Singh S, Köpke U, Howard CQ , Petersen D. Analyses of contact forces and vibration response for a defective rolling element bearing using an explicit dynamics finite element model. *Journal of Sound and Vibration*. 2014;333(21):p.5356–5377. <http://dx.doi.org/10.1016/j.jsv.2014.05.011>
7. Moazen Ahmadi A, Petersen D , Howard CQ. A nonlinear dynamic model of the vibration response of defective rolling element bearings. *Proc of Australian Acoustics*; 2013;Victor Harbor, Australia 2013.
8. Zhao S, Liang L, Xu G, Wang J , Zhang W. Quantitative diagnosis of a spall-like fault of a rolling element bearing by empirical mode decomposition and the approximate entropy method. *Mechanical Systems and Signal Processing*. 2013 10//;40(1):p. 154-177.
9. Epps I , McCallion H. An investigation into the characteristics of vibration excited by discrete faults in rolling element bearings. *Annual Conference of the Vibration Association of New Zealand*; 1994;Christchurch.
10. Sapanen J , Mikkola A. Dynamic model of a deep-groove ball bearing including localized and distributed defects. Part 1: Theory. *Proceedings of the Institution of Mechanical Engineers, Part K: Journal of Multi-body Dynamics*. 2003;217(3):p. 201-211.
11. Sapanen J , Mikkola A. Dynamic model of a deep-groove ball bearing including localized and distributed defects. Part 2: Implementation and results. *Proceedings of the Institution of Mechanical Engineers, Part K: Journal of Multi-body Dynamics*. 2003;217(3):p. 213-223.
12. Sawalhi N , Randall R. Simulating gear and bearing interactions in the presence of faults: Part I. The combined gear bearing dynamic model and the simulation of localised bearing faults. *Mechanical Systems and Signal Processing*. 2008;22(8):p. 1924-1951.
13. Sawalhi N , Randall R. Simulating gear and bearing interactions in the presence of faults: Part II: Simulation of the vibrations produced by extended bearing faults. *Mechanical Systems and Signal Processing*. 2008;22(8):p. 1952-1966.
14. Cao M , Xiao J. A comprehensive dynamic model of double-row spherical roller bearing—Model development and case studies on surface defects, preloads, and radial clearance. *Mechanical Systems and Signal Processing*. 2008;22(2):p. 467-489.
15. Sassi S, Badri B , Thomas M. A numerical model to predict damaged bearing vibrations. *Journal of Vibration and Control*. 2007;13(11):p. 1603-1628.
16. Tadina M , Boltežar M. Improved model of a ball bearing for the simulation of vibration signals due to faults during run-up. *Journal of Sound and Vibration*. 2011;330(17):p. 4287-4301.

17. Harsha SP. Nonlinear dynamic analysis of an unbalanced rotor supported by roller bearing. *Chaos, Solutions & Fractals*. 2005 10//;26(1):p. 47-66.
18. Harsha SP. Nonlinear dynamic analysis of a high-speed rotor supported by rolling element bearings. *Journal of Sound and Vibration*. 2006 2/21//;290(1-2):p. 65-100.
19. Harsha SP, Sandeep K , Prakash R. Non-linear dynamic behaviors of rolling element bearings due to surface waviness. *Journal of Sound and Vibration*. 2004 5/6//;272(3-5):p. 557-580.
20. Harsha SP , Kankar PK. Stability analysis of a rotor bearing system due to surface waviness and number of balls. *International Journal of Mechanical Sciences*. 2004 7//;46(7):p. 1057-1081.
21. Harsha SP, Sandeep K , Prakash R. The effect of speed of balanced rotor on nonlinear vibrations associated with ball bearings. *International Journal of Mechanical Sciences*. 2003 4//;45(4):p. 725-740.
22. Moazen Ahmadi A, Petersen D , Howard CQ. A nonlinear dynamic vibration model of defective bearings – The importance of modelling the finite size of rolling elements. A nonlinear dynamic vibration model of defective bearings – The importance of modelling the finite size of rolling elements. 2015. <http://dx.doi.org/10.1016/j.ymsp.2014.06.006>
23. Tandon N , Choudhury A. A theoretical model to predict the vibration response of rolling bearings in a rotor bearing system to distributed defects under radial load. *Journal of Tribology*. 2000;122(3):p. 609-615.